Laboratory Characterization of Direct Readout Si:Sb and Si:Ga Infrared Detector Arrays

Mark E. McKelvey, Nicolas N. Moss, Robert E. McMurray, Jr.,
John A. Estrada, John H. Goebel, Craig R. McCreight
NASA Ames Research Center, Moffett Field, CA 94035

Maureen L. Savage
Sterling Software Inc., 1121 San Antonio Road, Palo Alto, CA 94303

Frank Junga, Thomas Whittemore
Lockheed Research Laboratory, 3251 Hanover Street, Palo Alto, CA 94304

Abstract

Highlights of recent results obtained at Ames Research Center in performance evaluations of infrared detector arrays are presented. Antimony- and gallium-doped silicon direct readout 58x62 element hybrid devices from Ames' ongoing detector technology development program are described. The observed characteristics meet most of the performance goals specified by the SIRTF instrument teams and compare favorably with the best performance reported for discrete non-integrating extrinsic silicon detectors. Initial results of radiation-environment testing are reported, and non-ideal behavior demonstrated by these test devices is discussed.

Introduction

Space-based infrared (IR) astronomy projects such as NASA's Space Infrared Telescope Facility (SIRTF) and Large Deployable Reflector (LDR) and the European Space Agency's Infrared Space Observatory (ISO) will require significant advances in detector technology if they are to realize the full potential offered by on-orbit observing conditions. A continuing technology development program has been underway at Ames Research Center to help achieve sufficient improvements in the state of the art to allow space telescope IR observations to achieve sensitivity limited only by the natural background flux.

As part of this work, evaluations have been carried out in some detail on two 58x62 element IR detector array types based on the Hughes Aircraft Company's CRC-228 direct readout multiplexer[1,2]. Si:Sb and Si:Ga detector substrates have been indium-bump-bonded to the CRC-228 to produce high performance hybrid arrays. The Infrared Array Camera[3] (IRAC) for SIRTF has specified these devices as baseline candidate technologies for two of its wavelength bands.

A photograph of one of the arrays is shown in Fig. 1, and a schematic of the array unit cell is shown in Fig. 2. Each unit cell contributes one detector element to each of the two parallel output channels when its unique address is sent to the on-chip decoder circuit. The unit cell is repeated 58x31 times to make up the full array of 3596 pixels. A software-selectable reset pulse can be applied during the address period to reset the integration nodes in a unit cell to a known reference level. Alternately, a non-destructive read can be performed, allowing several measurements to be made of the charge packet as it builds up during the integration period.

In the following sections, recent measurements of the basic performance of these devices will be highlighted, radiation testing procedures will be outlined, and limitations of these arrays will be briefly discussed.

Performance

Table 1 contains a summary of the various figures of merit obtained to date on the two array types tested. The read noise figure for the Si:Ga array is superior to that listed for the Si:Sb type, but this is largely an artifact of the more recent (and improved) test methods used in the evaluation of the gallium-doped array. Because the Si:Ga array was loaned to us for a limited time by NASA's Goddard Space Flight Center[4], it was the device most recently tested. Since the return of the Si:Ga array, our attention has shifted back to the Si:Sb device, and upcoming tests are expected to show read noise comparable to that of the Si:Ga array.

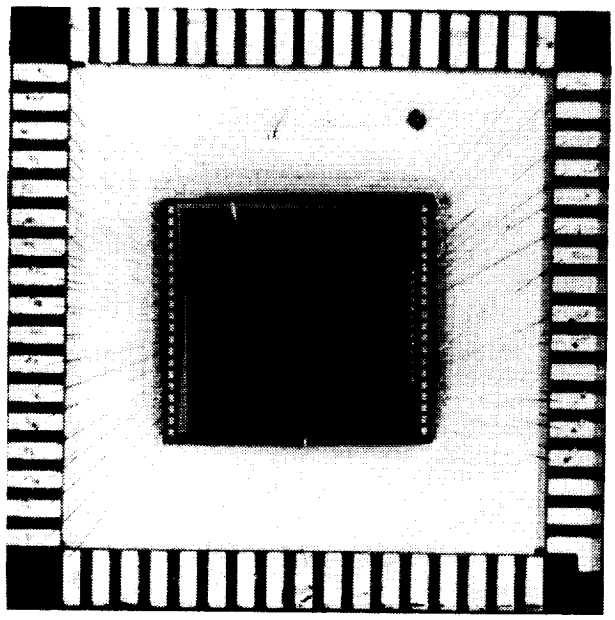

Figure 1. 58x62 DRO infrared detector array.

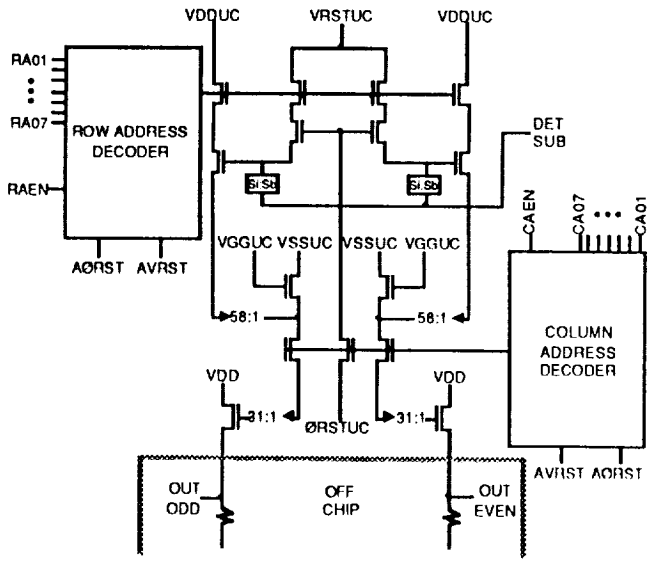

Figure 2. Schematic diagram of multiplexer unit cell.

Characteristic	Si:Sb		Si:Ga	Units	Conditions
General					
Dopant Concentration	4		40(?)	10^{15} atoms/cm^3	
Format		58 x 62		rows x columns	
Pixel size		75		µm	Square
Pixel Spacing		75		µm	Centers
Wavelength range	15 - 31		4 - 18	µm	
Test background	0.17 - 18		0.30 - 28	10^4 ph/s	Corrected to
	0.30 - 32		0.54 - 50	10^8 ph/cm^{2}s	response peak
Performance					
Responsivity	3.8		12	A/W	8 K, 2V bias (70V Si:Ga)
Read noise	220		95	µVrms	q_b=1.8 x 10^5 ph/s
	100		53	rms e$^-$	(2.8 x 10^5 ph/s Si:Ga)
NEP	2.7		0.24	10^{-17} W/√Hz	t_i = .204 s
Gη product	0.17		0.99(?)		-
Dark current	13		450	e$^-$/s	8 K, 1 V bias (7K,70V Si:Ga)
	3.2		75	aA	q_b = zilch
Input Capacitance	0.06		0.07	pF	Measured
Well Capacity	>2		>5	10^5 e$^-$	
Max. integration time	>10^4		>10^3	s	8 K, dark current limited
Operating temperature		5 - 12		K	
Uniformity	15		8	%	1σ/mean

Table 1. 58x62 DRO array test summary.

The performance summarized in Table 1 compares well with IRAC goals in most areas, and indeed with the best reported non-integrating discrete detector performance. The one area shown that is out of the IRAC specification is the dark current measured for the Si:Ga array at 450 e$^-$/s. This is well above the specified 10 e$^-$/s, but still is low enough to give a dark-

current-limited maximum integration time (t_i) of $>10^3$ s. Actually, the cosmic ray background flux, rather than the dark current, is likely to limit t_i on SIRTF.

Pixel-to-pixel uniformity is good in both array types with variations in responsivity of 8% for the Si:Ga array and 15% for the Si:Sb array (defined as standard deviation/mean). These levels produce obvious nonuniformities in the raw signal output, but they can be corrected without difficulty in post-processing.

The dependence of Si:Ga response and noise on the applied bias voltage is shown in Fig. 3. Responsivity is nearly proportional to applied bias between 20 V and 60 V, and becomes superlinear at higher biases. The read noise is essentially independent of bias below 70 V, but noise behavior is erratic at higher applied voltages. A definite impact-ionizing breakdown condition is not achieved in the Si:Ga below 95 V (the maximum available in our test setup), but low noise performance is not repeatably obtainable above 70 V (1400 V/cm). At 70 V applied bias and a temperature of 8 K, peak responsivity in the Si:Ga array is 12 A/W and read noise is 53 e^- rms. This corresponds to a read-noise limited NEP of 2.4 x 10^{-18} W/$\sqrt{Hz}$ in a 217 ms integration period. The best measured NEP for the Si:Sb array is an order of magnitude higher, but this should improve by a factor of two when its read noise is measured in our improved test set.

An unexpected variation in Si:Ga responsivity with operating temperature was observed and is shown in Fig. 4. A steep decrease in responsivity with increasing temperature above 7 K was noticed near the end of our Si:Ga tests. Improved mobility due to a decrease in charged impurity scattering should occur as temperature is increased, which should create a modest increase in responsivity at higher operating temperatures. This trend is observed for the Si:Sb array to temperatures >12 K, and in the Si:Ga array for temperatures up to 7 K. The curious drop in Si:Ga response above 7 K is not understood, but could be explained by the presence of a very shallow energy level (~ few meV) that contributes long-wavelength photoconductivity at low temperatures but is thermally depopulated as temperature is increased. An attempt was made to

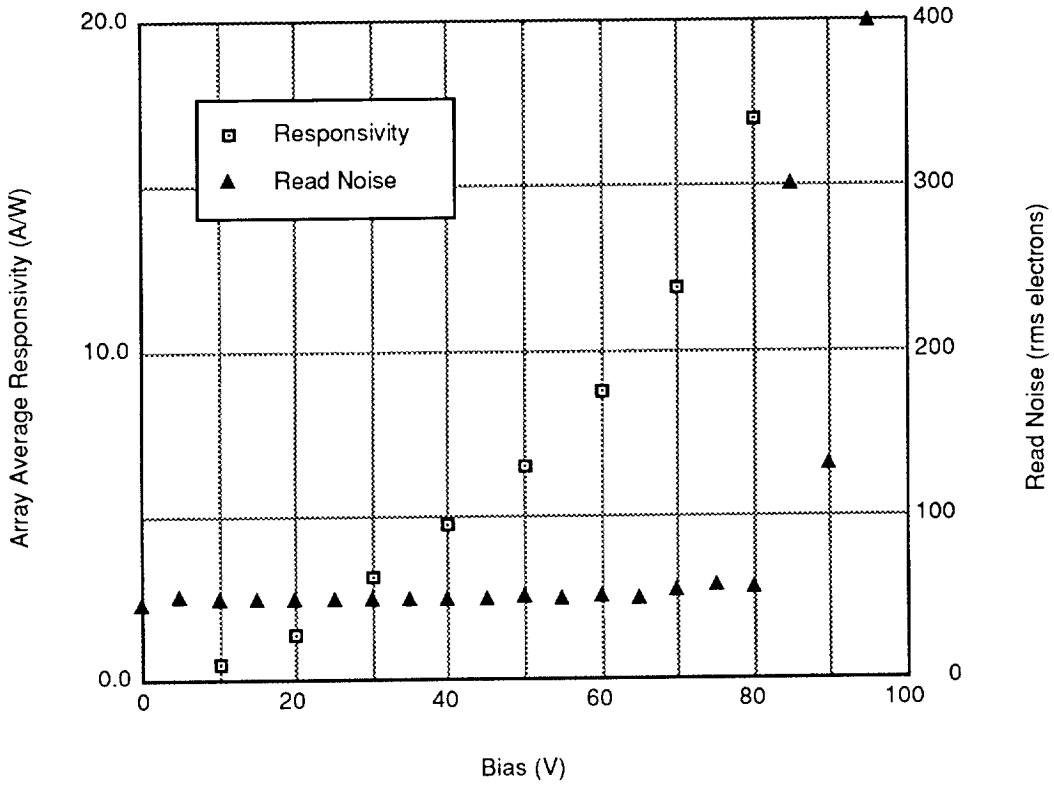

Figure 3. Si:Ga array responsivity and read noise vs. applied bias voltage. Background = 3 x 10^3 ph/pixel-s. T = 8 K. Integration time = 217 ms.

demonstrate long wavelength photoconductivity in the Si:Ga array by blocking wavelengths shorter than 20 μm, but no photoresponse was observed in this test. This does not rule out the shallow levels, since the effect may depend on the spectral quality of the incident radiation (particularly if the supposed level was an excited state of the Ga dopant).

The presence of very shallow levels may also be suggested by the dependence of Si:Ga dark current on temperature, shown in Fig. 5. The activation energy obtained from this Arrhenius plot is on the order of a few meV, much less than the 72 meV expected if thermal activation of the Ga impurity controlled the dark current. The two regimes evident in the plot differ in activation energy by nearly a factor of two. This might be consistent with a single level and a change from diffusion- to generation-recombination-limited carrier transport.

A systematic determination of the cause of the responsivity decrease above 7 K and the small dark current activation energy was not possible within the time available. If long wavelength photoconductivity is contributing to the responsivity below 7 K, the quoted responsivity is in error. A careful measurement of spectral response would be required before detector material displaying this behavior could be used on a space telescope mission.

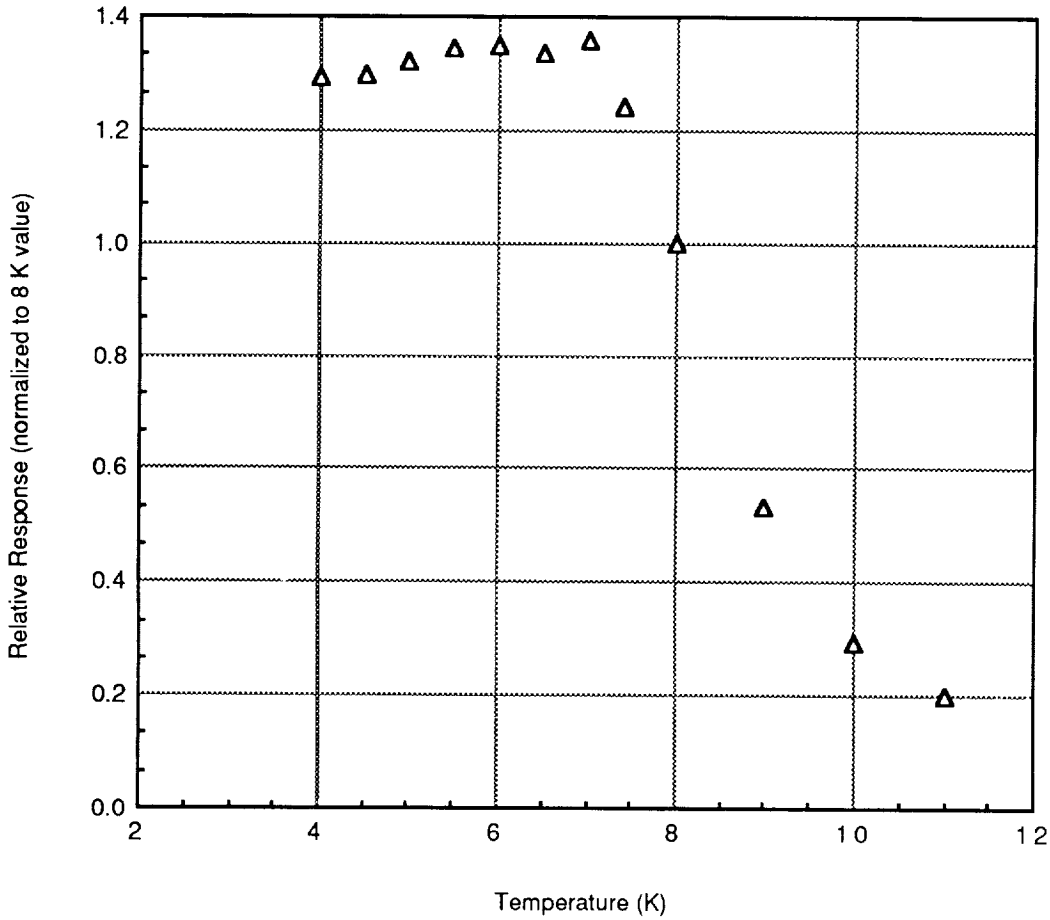

Figure 4. Si:Ga array relative responsivity vs. temperature, normalized to 8 K value (12 A/W). Background = 4 x 10^3 ph/pixel-s. Integration time = 217 ms.

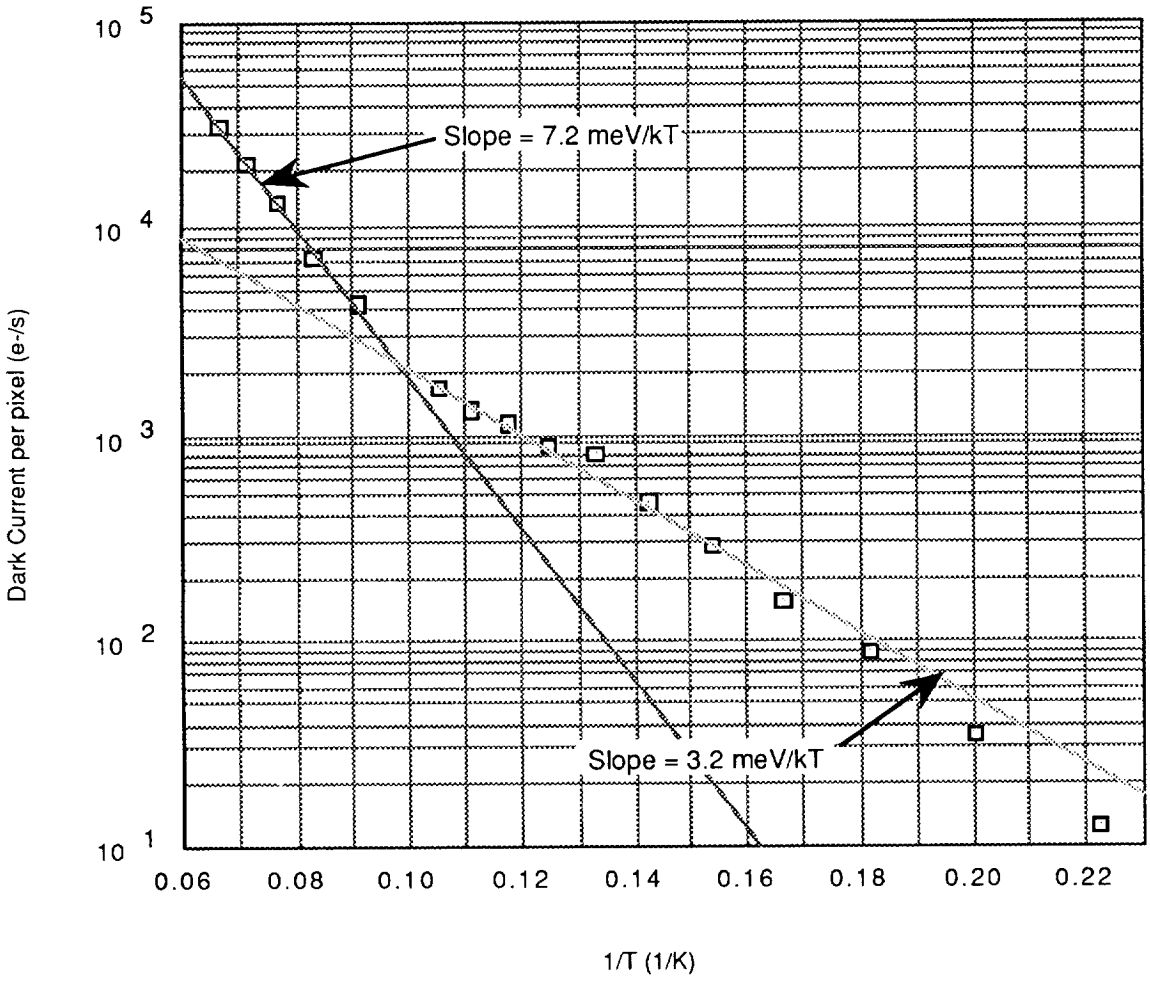

Figure 5. Si:Ga array dark current vs. temperature.

Radiation Testing

Space telescope platforms will experience a cosmic ray background composed primarily of high energy protons. The level of this background will depend on the orbit chosen, but representative predictions are for a proton flux of about 4 p^+/cm^2-s over most of a high (70,000 km) orbit[5]. "Pockets" of higher flux levels will be encountered with rates increased by up to two orders of magnitude.

Laboratory detector testing in an ionizing radiation environment is required to understand what changes in performance characteristics will occur and what strategies can be used to maintain the best possible radiometric calibration. To this end, tests of these detector arrays in γ-ray and proton environments have been initiated and constitute a major focus for near-term testing at Ames.

Although γ-rays constitute only a fraction of the on-orbit ionizing radiation environment, the convenience of small radioactive γ-sources that can be safely used in laboratory tests makes them attractive for preliminary investigations. ^{137}Cs, ^{241}Am, and ^{55}Fe sources of activities up to 10 mCi have been mounted inside our test cryostat to yield dose rates up to 0.3

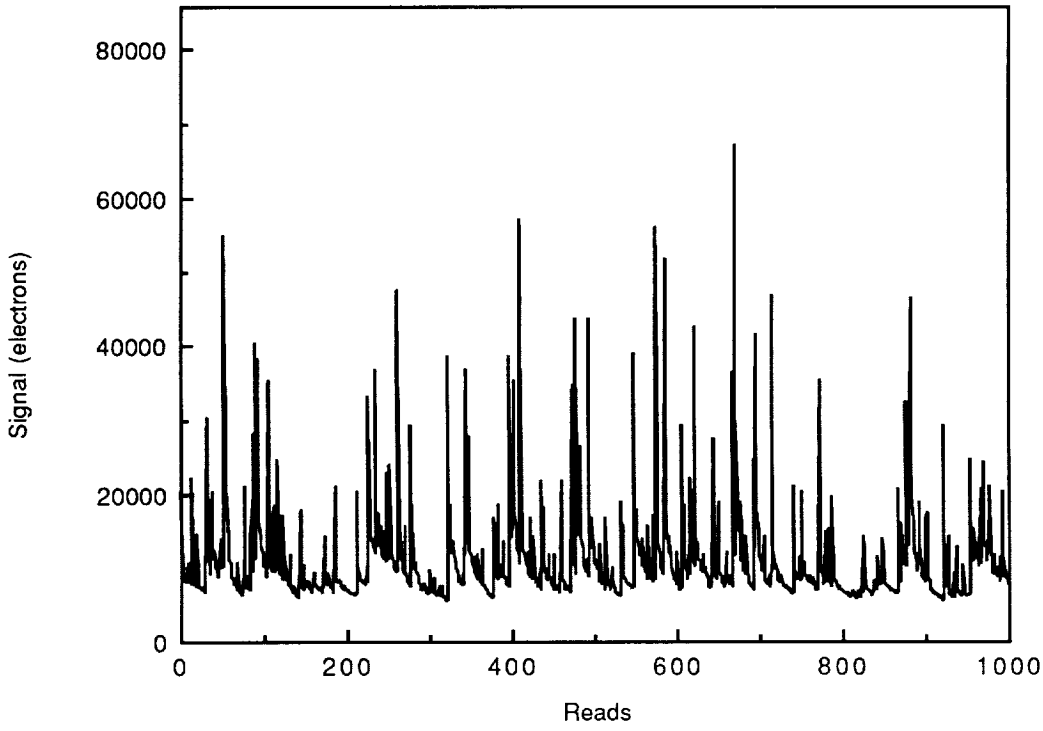

Figure 6. Si:Sb response in γ-environment. ^{137}Cs (660 keV) irradiation. Read rate = 60 Hz. T = 8 K. Bias = 2 V.

rad(Si)/hr in the detector arrays. Although these dose rates are much lower than the worst on-orbit conditions, they do produce doses sufficient to significantly change detector performance characteristics. Experimentation with different annealing schemes to recover the pre-irradiation calibration is also possible in our in-house tests.

Figs. 6 and 7 are representative of data gathered in initial radiation testing of these devices. Fig. 6 is a time series of a single Si:Sb pixel output under ^{137}Cs γ-ray bombardment at a calculated dose rate of 0.2 rad(Si)/hr. Fig. 7 is a pulse height distribution of the same data, showing a peak at about 5,000 carriers/read and a characteristic pseudo-exponential tail. Some hits produce in excess of 60,000 carriers. While these events produce only a fraction of the number of carriers associated with high energy proton interactions, they are sufficient to cause shifts in charge distribution leading to changes in responsivity and perhaps dark current, although the latter has not been demonstrated in these devices.

Such a shift in responsivity is shown in Fig. 8. The lower curve in Fig. 8 shows the change in Si:Ga array average responsivity during the deposition of about 1 rad(Si) at an IR background of about 5 x 10^4 ph pix^{-1} s^{-1} and a temperature of 8 K. After a six-hour irradiation under these conditions responsivity had increased by about 7 %. Once the Cs source was removed, a natural recovery began with a time constant on the order of several hours. Actual astronomical observations would clearly require some kind of intervention to restore the photometric calibration of the device for efficient use of allotted observing time. Boosting the bias level beyond breakdown to flood the material with free carriers has been shown to remove the radiation-induced responsivity shift in other devices. However, this did not occur for the maximum 95 V bias (1900 V/cm) our test system could supply to the Si:Ga array. A short-duration thermal cycle to 20 K did recover the initial performance, and could be reasonably performed on-orbit with a properly designed array mount.

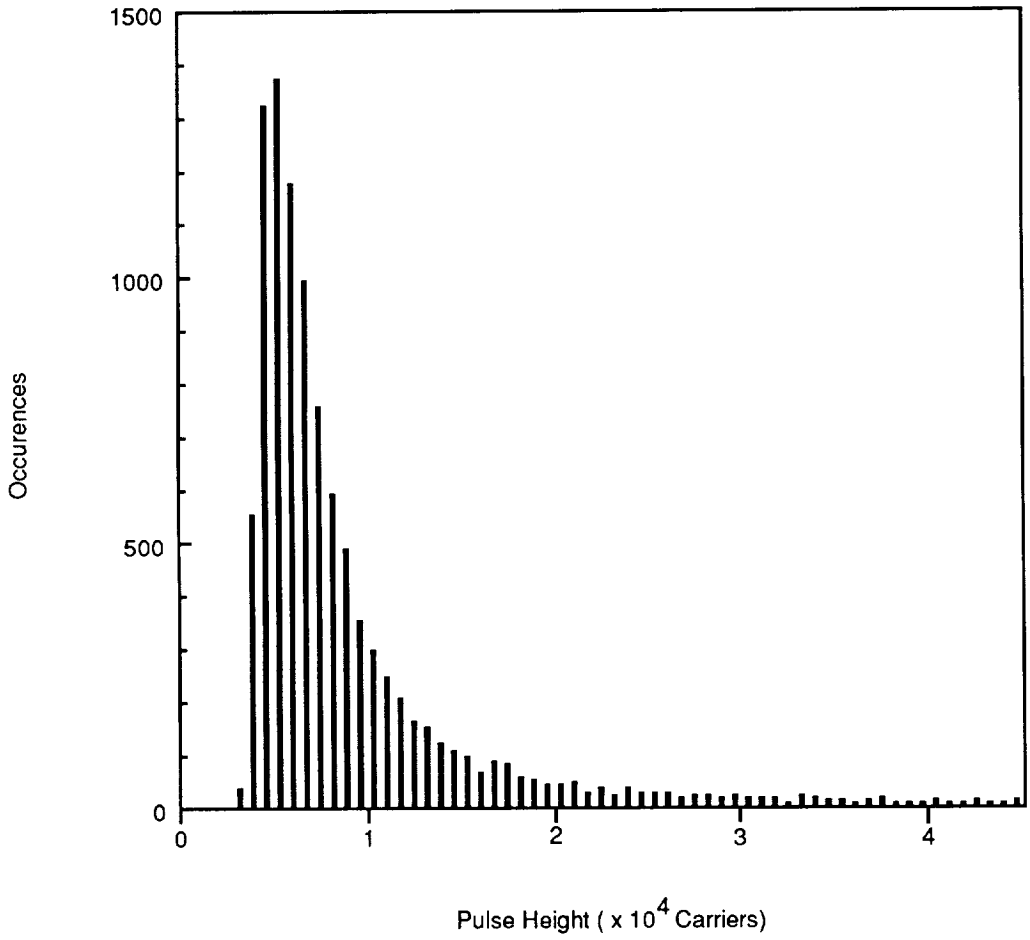

Figure 7. Si:Sb γ-ray pulse height distribution. ^{137}Cs (660 keV) irradiation. T = 8 K. 2k total reads.

The upper curve in Fig. 8 shows results of a similar irradiation of the Si:Sb array. Here the responsivity shift is much larger, showing a near doubling at an accumulated dose of 1 rad(Si) and a similarly long natural recovery period. The difference in the magnitude of responsivity change between the Si:Sb array and its Si:Ga counterpart is likely due to the higher level of impurity compensation (through the unintended presence of boron) in the n-type Sb material. Actual shifts in response depend on dose rate and IR background level, and perhaps on applied bias and operating temperature. Mapping out the effects of these and other factors will be carried out in future work.

Because the on-orbit environment is primarily composed of high energy protons, a better simulation can be made with a proton source such as a particle accelerator. Arrangements have been made in conjunction with Lockheed Research Laboratory to study array performance under proton bombardment at the 74-inch Crocker Cyclotron on the campus of the University of California at Davis. Flux levels down to 5 $p^+cm^{-2}s^{-1}$ at energies up to 67 MeV can be obtained, and tests in various simulated space telescope environments are to begin shortly.

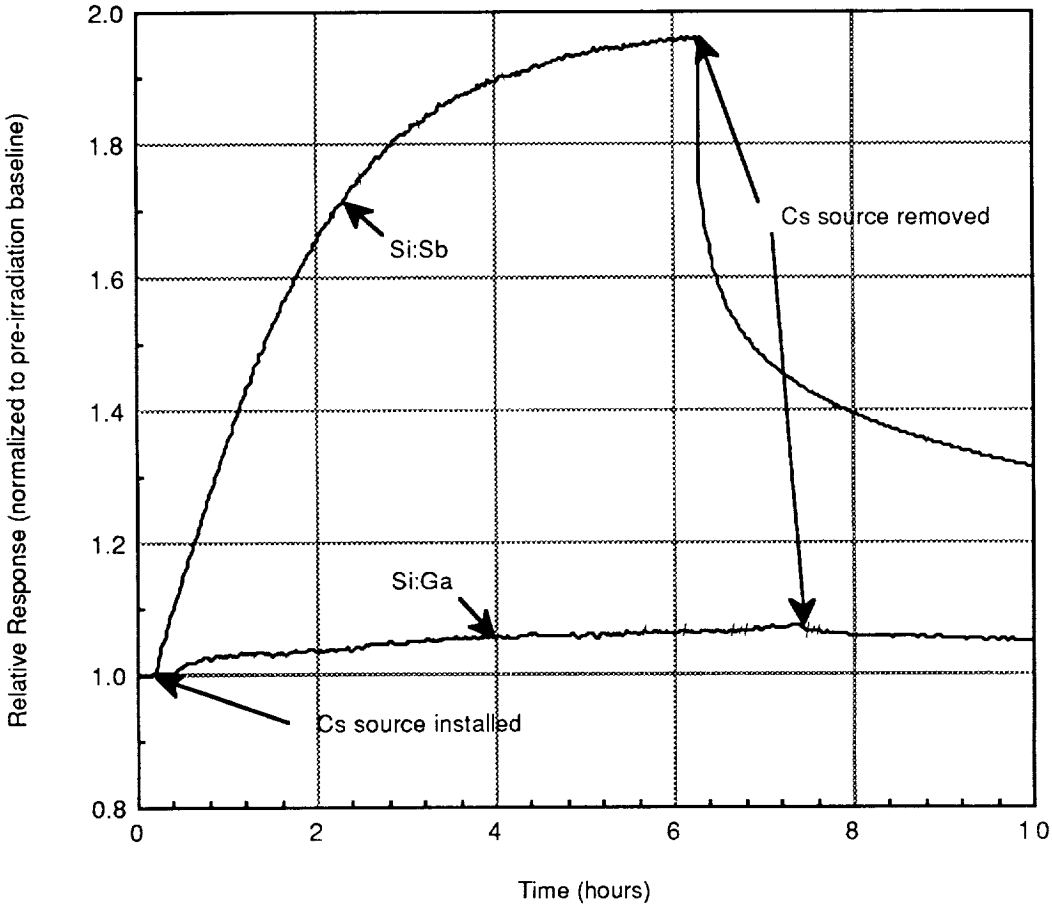

Figure 8. Si:Ga and Si:Sb responsivity under γ-radiation. ^{137}Cs (660 keV) source, 0.183 rad(Si)/hr. T = 8 K. Background = (a) 4.8 x 10^4 and (b) 9.0 x 10^3 ph/pix-s.

Problem Areas

While these arrays have generally delivered a high level of performance, some problem areas have become apparent. As bulk photoconductors, these arrays have shown some of the anomalous behavior characteristics long associated with this type of detector[6]. Multiple time constants, hook anomalies, and memory effects have been observed in these devices and represent serious limitations in astronomical applications. Fig. 9 shows the time development of the output of a single Si:Ga pixel under various step changes in incident IR flux. The time constant problems worsen as the flux level is decreased, and this may be a critical obstacle in the ultra-low background conditions anticipated in space telescope applications. Materials processing, detector design, or other operational improvements may lessen the severity of these non-ideal characteristics. Determining whether such techniques can sufficiently mitigate these concerns is a major objective of the Ames detector development program.

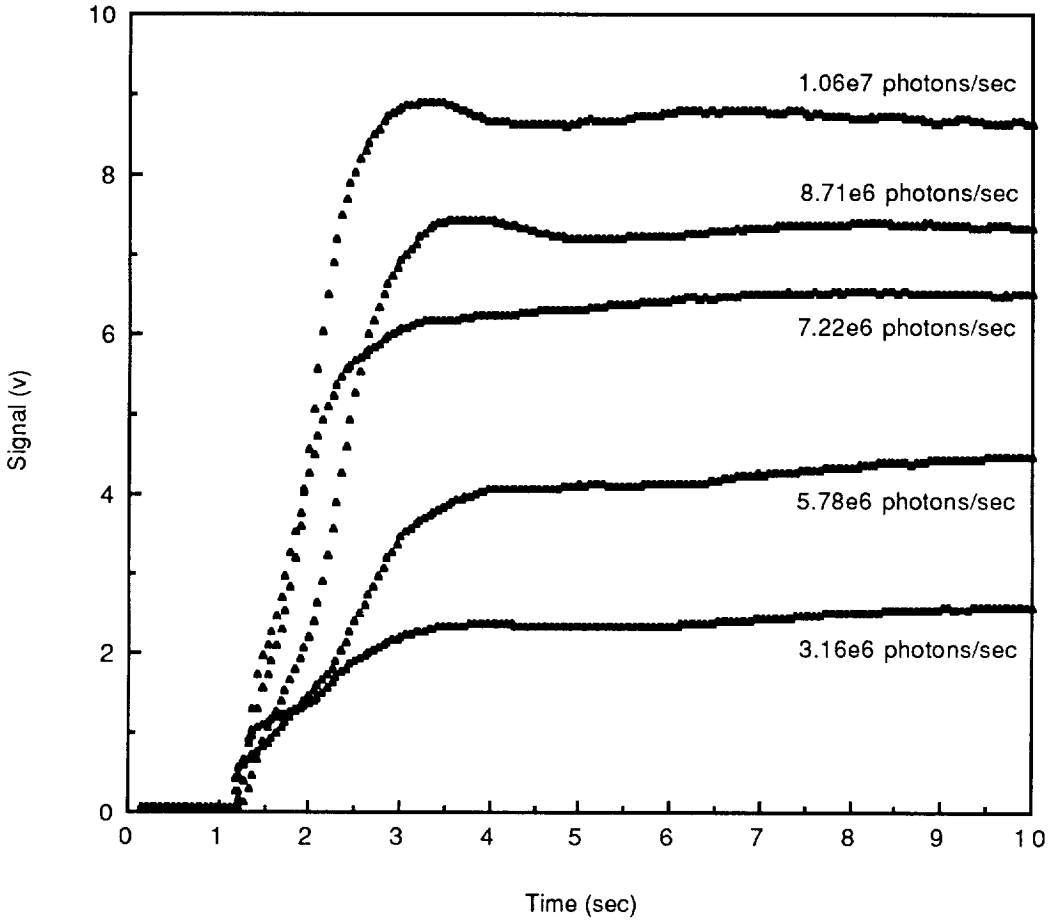

Figure 9. Si:Ga single pixel response to step changes in IR flux level. Gain = 40. Zero signal = cold slide in field of view. T = 8 K.

Summary

Characterization of Si:Sb and Si:Ga 58x62 direct readout IR detector arrays has been carried out in considerable detail. These devices have shown excellent performance characteristics overall. They meet or exceed most IRAC specifications for detector figures of merit, with the exception of certain transient response criteria. The performance demonstrated by these arrays also compares well with discrete detectors in the same wavelength range. Radiation environment testing has shown shifts in responsivity after γ-ray bombardment as expected. These shifts vary in magnitude with incident IR background and other parameters. Thermal annealing has proven effective in restoring pre-irradiation performance levels.

The observed slow transient behavior may prove to be a serious limitation in space astronomical applications. These anomalies are familiar from previous experience with bulk photoconductors. The Infrared Astronomical Satellite (IRAS) successfully used bulk photoconductors at low background, and improvements in materials processing and operating techniques may be able to surmount the present difficulties for applications such as SIRTF. Alternatively, other detector technologies (such as impurity band conduction (IBC) detectors[7]) may prove more suitable for these missions.

Much work remains before a final determination of the suitability of these array types can be made. Future test work is planned to further quantify the transient characteristics of these devices and to add to the (inadequate) existing database on their performance in a radiation environment.

---

[1]McKelvey, M. E. *et al.*, *Proc. Soc. Photo-Opt. Instrum. Eng.* **868**, 73 (1987).
[2]Orias, G. and Campbell, D., NASA Contractor Report 177,446 (1986).
[3]G. G. Fazio *et al.*, *Proc. Soc. Photo-Opt. Instrum. Eng.* **589**, 229 (1986).
[4]G. Lamb *et al.*, in Infrared Astronomy with Arrays (C. G. Wynn-Williams and E. E. Becklin, eds.), University of Hawaii, 144 (1987).
[5]E. G. Stassinopolous, NASA SP-3054 (1970).
[6]Zachor, A. S., and Huppi, E. R., Appl. Opt. **20**, 1000 (1981).
[7]T. Herter, C. E. Fuller, G. E. Gull, and Houck, J. R., in Infrared Astronomy with Arrays (C. G. Wynn-Williams and E. E. Becklin, eds.), University of Hawaii, 128 (1987).